THE JOURNAL OF BIOLOGICAL CHEMISTRY VOL. 281, NO. 10, pp. 6455–6462, March 10, 2006

Membrane Topology of the Transporter Associated with Antigen Processing (TAP1) within an Assembled Functional Peptide-loading Complex*[S]

Received for publication, September 6, 2005, and in revised form, December 2, 2005 Published, JBC Papers in Press, January 5, 2006, DOI 10.1074/jbc.M509784200

Susanne Schrodt, Joachim Koch, and Robert Tampé[1]

From the Institute of Biochemistry, Biocenter, Goethe-University Frankfurt, Marie-Curie-Strasse 9, D-60439 Frankfurt/Main, Germany

The transporter associated with antigen processing (TAP) translocates antigenic peptides from the cytosol into the endoplasmic reticular lumen for subsequent loading onto major histocompatibility complex (MHC) class I molecules. These peptide-MHC complexes are inspected at the cell surface by cytotoxic T-lymphocytes. Assembly of the functional peptide transport and loading complex depends on intra- and intermolecular packing of transmembrane helices (TMs). Here, we have examined the membrane topology of human TAP1 within an assembled and functional transport complex by cysteine-scanning mutagenesis. The accessibility of single cysteine residues facing the cytosol or endoplasmic reticular lumen was probed by a minimally invasive approach using membrane-impermeable, thiol-specific fluorophores in semipermeabilized "living" cells. TAP1 contains ten transmembrane segments, which place the N and C termini in the cytosol. The transmembrane domain consists of a translocation core of six TMs, a building block conserved among most ATP-binding cassette transporters, and a unique additional N-terminal domain of four TMs, essential for tapasin binding and assembly of the peptide-loading complex. This study provides a first map of the structural organization of the TAP machinery within the macromolecular MHCI peptide-loading complex.

The adaptive immune system plays an essential role in protecting vertebrates against a broad spectrum of pathogens. The MHC[2] class I-dependent pathway of antigen presentation represents an elegant strategy to identify and eliminate infected or malignantly transformed cells, taking advantage of the constant turnover of endogenous proteins by the 26 and/or 20 S proteasome in the cytosol. A minor fraction of the resulting peptides is translocated by the transporter associated with antigen processing (TAP) into the ER lumen and is subsequently loaded onto MHC class I molecules. These peptide-MHC complexes are then shuttled to the cell surface where they are inspected by cytotoxic T-lymphocytes. MHC class I molecules loaded with "non-self" peptides can trigger lysis or apoptosis of the infected or malignant cell (1, 2).

TAP is a member of the ATP-binding cassette (ABC) protein superfamily, which uses ATP to translocate a large variety of solutes across biological membranes (3, 4). The minimal functional unit of an ABC transporter requires two transmembrane domains (TMDs), which align the peptide-binding site and translocation pathway as well as two cytosolic nucleotide-binding domains, which energize substrate translocation across the membrane. In eukarya, these domains are organized either as a "full transporter" or as a homo- or heterodimeric "half-transporter." The ER-resident TAP complex is a heterodimer of TAP1 (81 kDa) and TAP2 (76 kDa), each composed of one TMD and one nucleotide-binding domain (5, 6). The TMD of each subunit can further be subdivided into a translocation core and a unique, extra N-terminal domain (7). The core TMD is essential and sufficient for heterodimerization, peptide binding, and peptide transport, whereas the N-terminal domain is required for tapasin binding and assembly of the multicomponent peptide-loading complex (7, 8).

X-ray structures of two bacterial ABC transporters have been solved at different resolutions, the lipid A flippase MsbA (9–11) and the vitamin B_{12} transporter $BtuC_2D_2$ (12). Strikingly, both ABC transporters display an entirely different organization of the TMDs with regard to the arrangement and number of TMs. Due to the difficulties obtaining well diffracting crystals, in particular of mammalian membrane proteins, biochemical techniques still represent the major tool to investigate their structure. In this respect, TAP is a challenge, as it is a multicomponent complex containing unique, largely extended TMDs.

Considerable progress has been made to determine the topology of membrane proteins, employing a variety of bioinformatics tools and experimental approaches, such as site-directed mutagenesis or reporter protein fusions. However, fusion of reporter molecules, such as β-lactamase, epitope tags, or glycosylation-targeting sequences, to truncated variants of ABC transporters often result in misintegrated and nonfunctional proteins. Moreover, because the length and hydrophobicity of TMs of ABC transporters are not well defined, prediction algorithms cause conflicting results. Taken together, the membrane topologies of ABC transporters, in particular TAP, are very difficult to predict and to approach experimentally.

In this study, we determined the membrane topology of TAP1 by a minimally invasive approach. Guided by hydrophobicity algorithms in combination with sequence alignments of TAP from different species and other members of the ABC-B subfamily, we introduced single cysteines into putative loops between transmembrane segments and probed for their accessibility toward labeling with thiol-specific, membrane-impermeable fluorescein-5-maleimide (FM). Labeling was performed in semipermeabilized cells. Here, we present for the first time the membrane topology of human TAP1 in a functional peptide transport complex within the ER membrane in a cellular context.

* This work was supported by the Deutsche Forschungsgemeinschaft (SFB 628). The costs of publication of this article were defrayed in part by the payment of page charges. This article must therefore be hereby marked "*advertisement*" in accordance with 18 U.S.C. Section 1734 solely to indicate this fact.

[S] The on-line version of this article (available at http://www.jbc.org) contains supplemental Fig. S1.

[1] To whom correspondence should be addressed. Tel.: 49-69-798-29475; Fax: 49-69-798-29495; E-mail: tampe@em.uni-frankfurt.de.

[2] The abbreviations used are: MHC, major histocompatibility complex; ABC, ATP-binding cassette; ConA, concanavalin A; DM, *n*-decyl-β-maltoside; FM, fluorescein-5-maleimide; TAP, transporter associated with antigen processing; TM, transmembrane helix; TMD, transmembrane domain; ER, endoplasmic reticular/reticulum; Ni-NTA, nickel-nitrilotriacetic acid; mAB, monoclonal antibody; i.m., intact membranes; per., permeabilized; AMS, 4-acetamido-4′-maleimidyl-stilbene-2,2′-disulfonic acid.

EXPERIMENTAL PROCEDURES

Cloning and Expression of Single-cysteine TAP Constructs—Human Cys-less *tap1* and *tap2* (13) were subcloned into pGem3Z or pCRScript, respectively. Cys-less *tap1* was cloned into the BamHI and HindIII sites of pFastBacDual™ (Invitrogen) downstream of the polyhedrin promoter. Cys-less *tap2* was cloned under the control of the p10 promoter into pFastBacDual.TAP1cys-less via XhoI and NsiI resulting in the plasmid encoding Cys-less TAP1 and TAP2 (pFastBacDual TAP1cys-less/TAP2cys-less).

Single cysteines were introduced into Cys-less TAP1 (S6C, A51C, A87C, S124C, S179C, S220C, F265C, S326C, T399C, S436C, and S488C) by site-directed mutagenesis. The following sense oligonucleotides were used: TAP1(S6C), 5′-GGCTTCCTCCAGATGTCCTGCTCCTAGA-3′; TAP1(A87C), 5′-GCTCCAAGTCCGAAAACTGTGGCGCTCAGG-3′; TAP1(S179C), 5′-GACTGCTGGGCTGTCTGGGTTCCG-3′; TAP1(F265C), 5′-CAGGGCGAAGTCTGCGGTGCCGTCCTGAG-3′; TAP1(T399C), 5′-TGCAGGAAATCAAGTGCCTGAACCAGAAGGA-3′; TAP1(S488C), 5′-ACCCCTAGATGTCCACCTAGTGGC-3′; TAP1(A51C), 5′-CCCTGCTGGTCCCTACCTGCCTGCCTCTG-3′; TAP1(S124C), 5′-CGCTCCCGGGTGTGCTGACTCCACCAGA-3′; TAP1(S220C), 5′-GCAGGATGGCTGTGCTGACACCTT-3′; TAP1(S326C), 5′-GTGGGGCTCCGTCTGCCTGACTATGGTGACCCTG-3′; and TAP1(S436C), 5′-GGCCAACTGGTGACCTGTGGCGCTGTGAGCTCTG-3′ (exchanged nucleotides are underlined). The identity of all constructs was confirmed by DNA sequencing. Single-cysteine constructs of TAP1 were combined with Cys-less TAP2 resulting in plasmids encoding both subunits (pFastBacDual.TAP1single-cys/TAP2cys-less).

Recombinant Baculovirus and Cell Culture—Bacmid DNA was produced by transformation of DH10Bac cells with the plasmids pFastBacDual.TAP1single-cys/TAP2cys-less according to the manufacturer's protocol (Invitrogen). Insect cells (*Spodoptera frugiperda*, *Sf9*) were grown in Sf900II medium (Invitrogen) following standard procedures. To generate recombinant baculovirus, *Sf9* insect cells were transfected with 5–10 μg of bacmid DNA using the BaculoGold transfection kit (BD Biosciences). For expression of single-cysteine constructs, cells were infected with recombinant baculovirus as described previously (14). Co-infections with tapasin were performed with a multiplicity of infection of three for the TAP constructs, and a multiplicity of infection of 30 for tapasin.

Peptide Transport Assays—The peptide RRYQNSTEL was radiolabeled with $Na^{125}I$ as described in Ref. 15. For radioactive transport assays, microsomes (100 μg of total protein) were resuspended in 50 μl of AP buffer (phosphate-buffered saline, 5 mM $MgCl_2$, pH 7.0) in the presence and absence of ATP (3 mM). Preparation of microsomes was performed as described previously (16). The transport reaction (50 μl) was started by adding 0.46 μM radiolabeled peptide for 3 min at 32 °C and terminated with stop buffer (phosphate-buffered saline, 10 mM EDTA, pH 7.0) on ice. After centrifugation, the microsomes were solubilized in lysis buffer (50 mM Tris/HCl, 150 mM NaCl, 5 mM KCl, 1 mM $CaCl_2$, 1 mM $MnCl_2$, 1% Nonidet P-40, pH 7.5) for 20 min on ice. N-core-glycosylated and thus transported peptides were recovered with concanavalin A (ConA)-Sepharose beads (Sigma) overnight at 4 °C. After washing with lysis buffer, ConA-bound peptides were quantified by γ-counting. A 200-fold molar excess of non-labeled RRYQKSTEL peptide or 20 μM herpes viral inhibitor ICP47 was used for competition of the TAP-specific peptide translocation.

To probe TAP function and membrane topology in parallel, insect cells (2.5×10^6) were semipermeabilized with 0.025% saponin (Sigma) for 1 min at 25 °C in 300 μl of HEPES buffer (50 mM HEPES, 140 mM NaCl, pH 7.0). After washing, the cells were resuspended in a final volume of 100 μl of AP buffer containing ATP (10 mM). The transport reaction was initiated with the fluorescent peptide RRYQNSTC(Φ)L (Φ indicates fluorescein coupled via a cysteine residue) at 0.46 μM and stopped after 3 min at 32 °C as described above. After lysis and binding to ConA beads, the glycosylated peptides were eluted with methyl-α-D-mannopyranoside (200 mM) and quantified with a fluorescence plate reader ($\lambda_{ex/em}$ = 485/520 nm; Polarstar Galaxy, BMG Labtech, Offenburg, Germany). Background transport activity was measured in the presence of apyrase (1 unit).

Thiol Accessibility Assay—*Sf9* insect cells (2×10^7) were harvested from shaking cultures 48 h after infection, washed once with HEPES buffer, and subsequently semipermeabilized with 0.025% saponin in HEPES buffer. Thiol-specific labeling of proteins was performed with 50 μM FM (stock in dry *N*,*N*-dimethylformamide, Molecular Probes) for 5 min at 25 °C in a final volume of 120 μl of HEPES buffer. The labeling reaction was stopped with β-mercaptoethanol (25 mM). After washing, the cells were solubilized on ice with 35 mM *n*-decyl-β-maltoside (DM, Glycon) in 120 μl of solubilization buffer (20 mM NaH_2PO_4, 140 mM NaCl, 15% glycerol, pH 7.4). For reference, the cells were permeabilized with 35 mM DM prior to labeling with FM. Insoluble material was removed by centrifugation at 100,000 × *g* for 30 min at 4 °C. The solubilized TAP complex was bound via the His_{10} tag of TAP1 to Ni-NTA-agarose (Qiagen), washed twice with washing buffer (phosphate-buffered saline, 15% glycerol, 3 mM DM, 20 mM histidine, pH 7.0), and eluted with histidine (100 mM) in washing buffer. Samples were analyzed by SDS-PAGE (10%). FM labeling was monitored by in-gel fluorescence using the Lumi-Imager F1™ (Roche Applied Science). Following transfer onto nitrocellulose, immunoblotting was performed with TAP1- (mAb148.3) and TAP2-specific (mAb435.3) antibodies (16, 17).

RESULTS

Function of the Cysteine-less TAP Complex—To light up the membrane topology of human TAP, Cys-less TAP subunits were generated by *de novo* gene assembly (13). We first studied whether the substitution of all 19 cysteines may affect transport function of the heterodimeric TAP complex. Cys-less *tap1* and *tap2* were combined in the baculovirus expression vector pFastBacDual to achieve expression of a Cys-less TAP heterodimer. Both subunits were expressed in insect cells as shown in Fig. 1*A*. Cys-less TAP1 and TAP2 display a slightly reduced electrophoretic mobility compared with wild-type subunits due to an additional C-terminal His_{10} tag and Strep tag for TAP1 and TAP2, respectively.

We then examined peptide transport of the Cys-less TAP complex using isolated microsomes and the radiolabeled peptide RR(^{125}I)YQNSTEL. N-core-glycosylated and thus translocated peptides were bound to ConA beads and quantified by γ-counting. As shown in Fig. 1*B*, Cys-less and wild-type TAP have almost the same ATP-dependent transport activity. Peptide translocation is peptide- and TAP-specific, as the transport activity is reduced to the background in the presence of an excess of non-labeled peptide (RRYQKSTEL) or the viral inhibitor ICP47 from herpes simplex virus (18). These results demonstrate the formation of a functional heterodimeric complex of Cys-less TAP1 and Cys-less TAP2.

Function of Single-cysteine TAP Complexes—To investigate the membrane topology of human TAP, we generated single-cysteine TAP1 constructs. Guided by sequence alignments as well as hydrophobicity algorithms of TAP from different species and related ABC transporters, 11 positions in loops between predicted transmembrane segments were chosen: S6C, A51C, A87C, S124C, S179C, S220C, F265C, S326C,

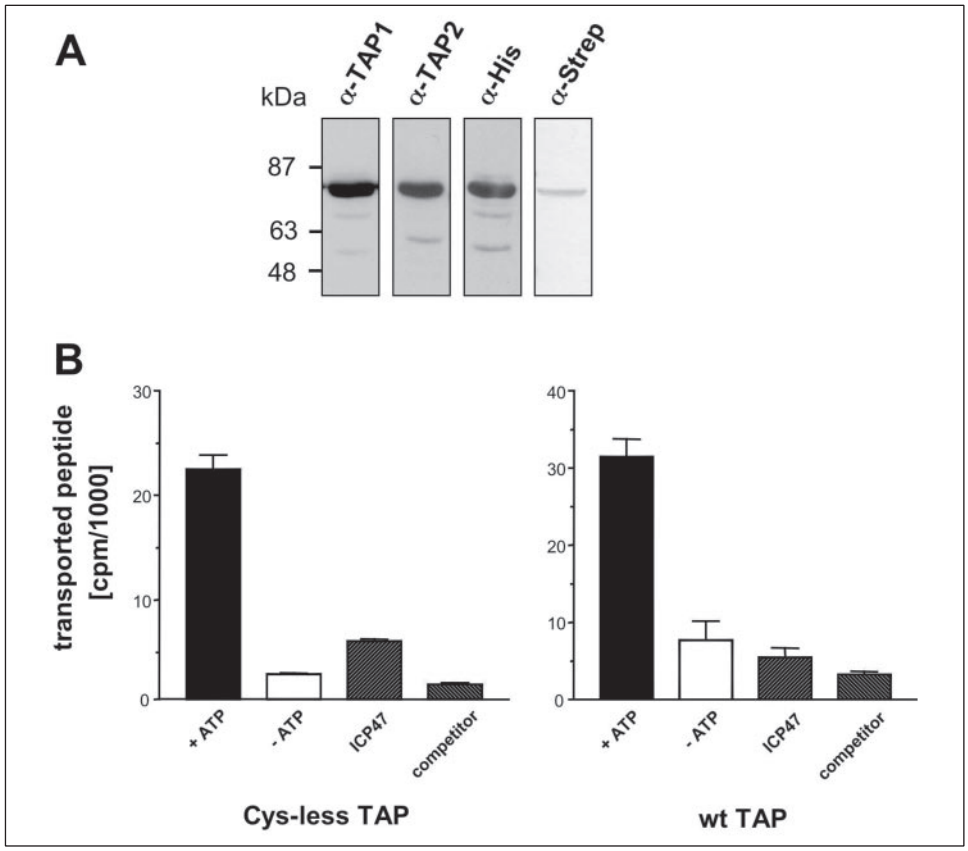

FIGURE 1. **Expression and function of Cys-less TAP.** *A*, expression of Cys-less TAP. Microsomes (20 μg of protein/lane) from baculovirus-infected insect cells were analyzed by SDS-PAGE (10%) followed by immunoblotting against TAP1 (mAb148.3, *α-TAP1*), TAP2 (mAb435.3, *α-TAP2*), the His_{10} tag at TAP1 (*α-His*), and the Strep tag at TAP2 (*α-Strep*). *B*, ATP-dependent peptide transport by Cys-less and wild-type TAP. The transport assay was performed with 0.46 μM radiolabeled peptide (RR(^{125}I)YQNSTEL) for 3 min at 32 °C in the presence (*black bars*) and absence (*open bars*) of Mg-ATP (3 mM) using Cys-less and wild-type TAP-containing microsomes (100 μg of total protein). N-core-glycosylated and therefore transported peptides were bound to ConA beads and quantified by γ-counting. Furthermore, transport assays were performed in the presence of the TAP-specific viral inhibitor ICP47 (20 μM, *right hatched bars*) or non-labeled competitor peptide (250-fold molar excess of RRYQKSTEL (*left hatched bars*). *Error bars* indicate the deviation of three independent experiments.

T399C, S436C, and S488C. To ensure co-expression of TAP1 and TAP2 within every infected cell, each single-cysteine TAP1 variant was combined with Cys-less TAP2 in the pFastBacDual vector. Cells were harvested early after infection (48 h) to preserve the cell morphology and to exclude effects because of over-expression.

To check whether the introduced single cysteines might interfere with TAP function, we analyzed the peptide translocation activity of all of the constructs in semipermeabilized cells with the fluorescent peptide RRYQNSTC(Φ)L. Similar to the assay described previously, N-core-glycosylated and thus transported peptides were bound to ConA beads and quantified after specific elution with methyl-α-D-mannopyranoside. As summarized in Fig. 2, all single-cysteine TAP complexes showed specific and ATP-dependent peptide transport. For most constructs, the transport efficiencies were similar to Cys-less TAP. Notably, the constructs S179C and S326C displayed even a slightly higher transport activity (130%), whereas the construct F265C exhibited 30% activity, when compared with Cys-less TAP. The expression levels of TAP1 and TAP2 were the same for most of the 12 TAP variants, as determined by immunoblotting (Fig. 2). Taken together, all single-cysteine complexes are functional and therefore suitable to investigate the membrane topology of TAP.

Membrane Topology Analyzed by Cysteine Accessibility—To establish a cysteine accessibility assay for an intracellular membrane protein complex, semipermeabilized cells were incubated with various concentrations of membrane-impermeable FM. After quenching of the reaction with β-mercaptoethanol, the cells were solubilized and the TAP complex was co-purified on Ni-NTA-agarose via the C-terminal His_{10} tag of TAP1 (Fig. 3, intact membranes, *i.m.*). As a control and reference, intracellular membranes were permeabilized (Fig. 3, *per.*) prior to labeling with FM. Fig. 3 summarizes the results obtained for in-gel fluores-

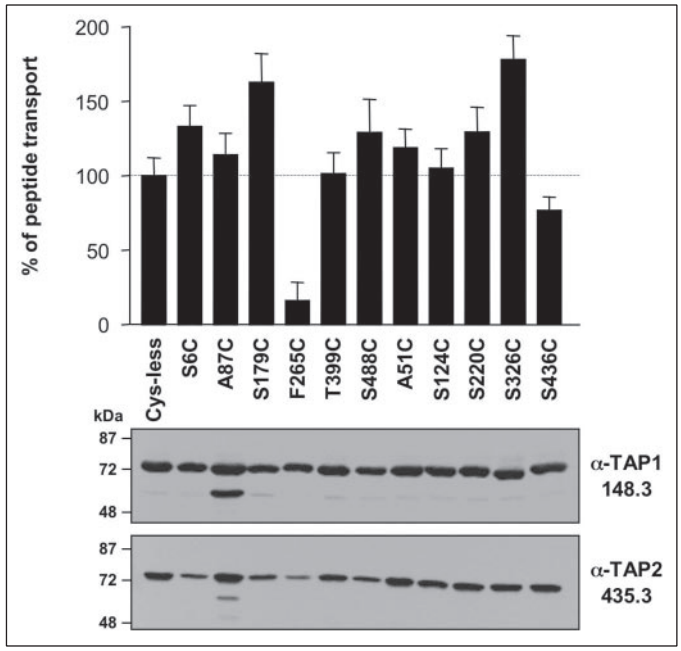

FIGURE 2. **Peptide transport of single-cysteine TAP mutants.** ATP-dependent peptide transport of single-cysteine TAP1 mutants was analyzed in semipermeabilized insect cells. The assay was performed with fluorescein-labeled peptide (0.46 μM, RRYQNSTC(Φ)L) for 3 min at 32 °C in the presence and absence of Mg-ATP (10 mM). N-core-glycosylated and therefore transported peptides were bound to ConA-beads and quantified by fluorescence detection after elution with methyl-α-D-mannopyranoside. The relative transport efficiencies of the single-cysteine TAP constructs are plotted in comparison to that of Cys-less TAP. The *error bars* indicate the deviation of three independent experiments. Aliquots (2×10^5 cells) used for the peptide transport assays were analyzed by SDS-PAGE (10%) and subsequent immunoblotting with TAP1- (mAb148.3) and TAP2-specific (mAb435.3) antibodies.

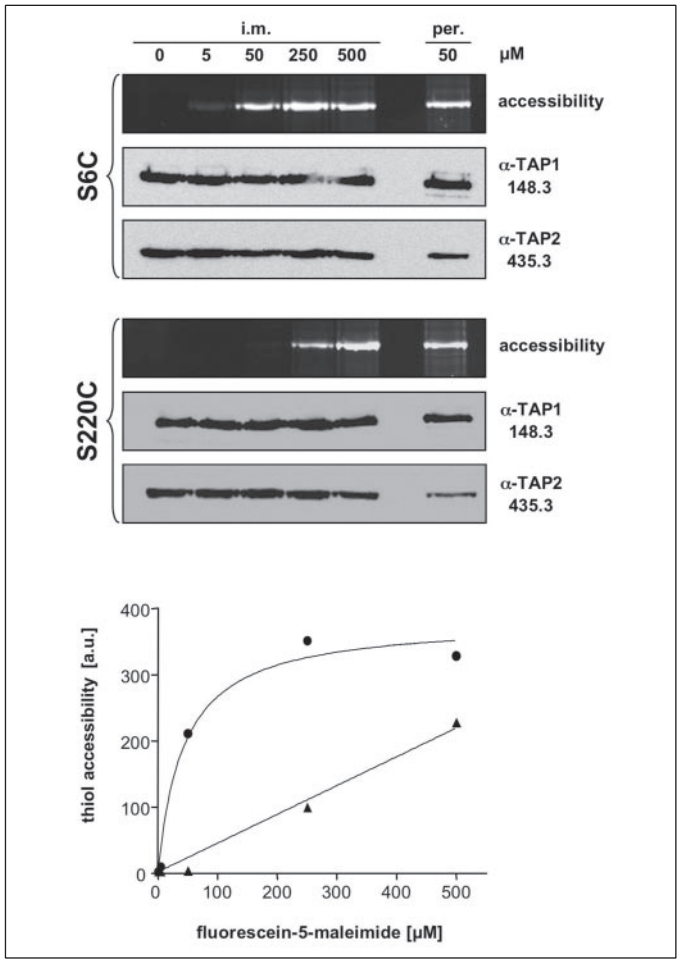

FIGURE 3. **FM labeling of single-cysteine TAP mutants.** Insect cells expressing single-cysteine AP variants (S6C or S220C of TAP1) were semipermeabilized with 0.025% saponin for 1 min at 25 °C and washed two times with HEPES buffer. Labeling was performed at different concentrations of FM (0–500 μM) for 5 min at 25 °C (intact membranes, *i.m.*). The labeling reaction was stopped with β-mercaptoethanol. As a reference, membranes were permeabilized (*per.*, 50) with DM prior to labeling with 50 μM FM. After labeling, the TAP complex was solubilized and purified via Ni-NTA-agarose. Aliquots were applied to SDS-PAGE (10%). FM labeling was monitored by in-gel fluorescence imaging. Co-purification of TAP1 and TAP2 was confirmed by immunoblotting with TAP1- (mAb148.3) and TAP2-specific (mAb435.3) antibodies, respectively. The relative accessibility of the single cysteines for FM labeling in intact membranes is plotted in dependence of the FM concentration. Values for the accessibility of S6C (●) and S220C (▲) are depicted from the intensities measured by in-gel fluorescence imaging. *a.u.*, arbitrary units.

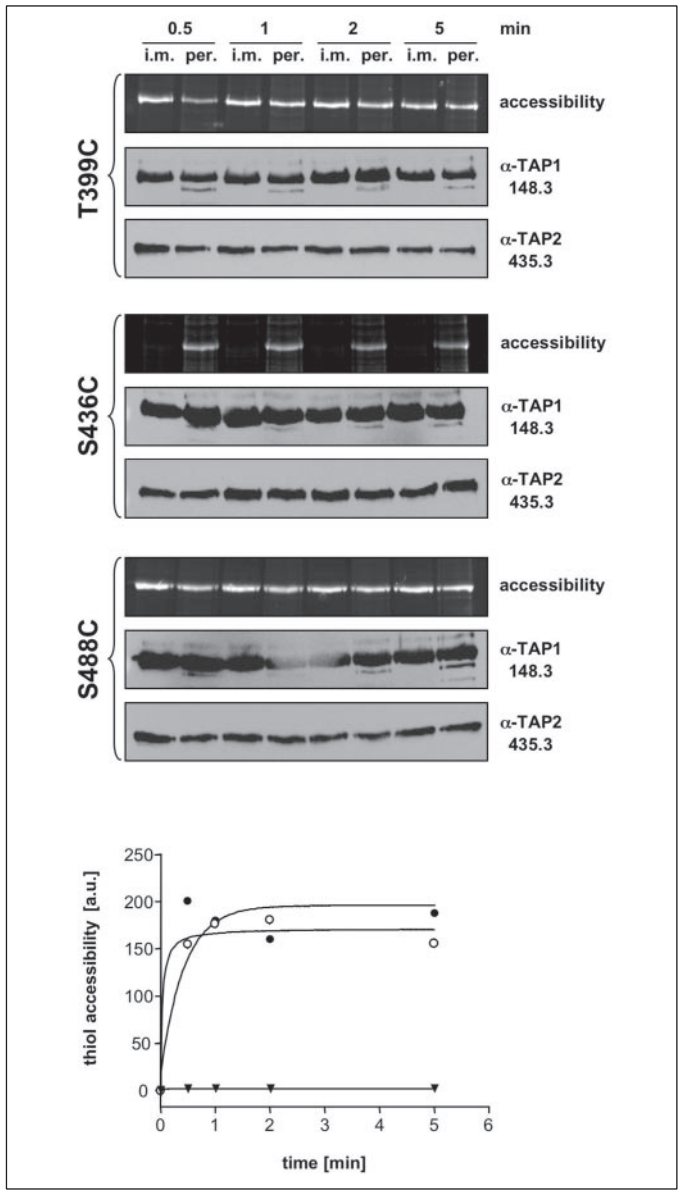

FIGURE 4. **Kinetics of FM labeling of single cysteines.** Semipermeabilized cells were labeled with FM (50 μM). The reaction was stopped with β-mercaptoethanol at different time points (0.5–5 min) (intact membranes, *i.m.*). For reference, membranes were permeabilized (*per.*) with DM prior to labeling. After labeling, the TAP complex was solubilized and purified via Ni-NTA-agarose. Aliquots were applied to SDS-PAGE (10%). FM labeling was monitored by in-gel fluorescence imaging. Co-purification of TAP1 and TAP2 was confirmed by immunoblotting with TAP1- (mAb148.3) and TAP2-specific (mAb435.3) antibodies, respectively. The relative accessibility of the single cysteines for FM labeling is plotted against the reaction time. Values for the accessibility of S488C (●), T399C (○), and S436C (▲) are depicted from the intensities in intact membranes measured by in-gel fluorescence imaging.

cence measurements and corresponding TAP1- and TAP2-specific immunoblots of the single-cysteine constructs S6C and S220C. Notably, the cysteine at position 6 (S6C) was already labeled at 5 μM FM. The reaction is site-specific, because Cys-less TAP shows no labeling even with a large excess of FM (500 μM, see also Fig. 5). The low concentration of FM sufficient for S6C labeling indicates that the N terminus is located in the cytosol. In contrast, the cysteine at position 220 displays a different reactivity. No specific labeling was detected with intact ER membranes at 5–50 μM FM, whereas aliquots permeabilized prior to labeling reacted quantitatively with the thiol-specific compound at a concentration of 50 μM. These results show that position 220 is located in the ER lumen. Notably, in the presence of a large excess of FM (250 μM), labeling was also detected within intact membranes, suggesting that, under these conditions, FM can cross the membrane. Treatment of the constructs S6C and S220C with the membrane-impermeable maleimide compound stilbene disulfonate maleimide (AMS) prior to labeling with FM confirmed the localization of the introduced cysteines. Labeling of the cysteine S6C is impeded when pre-incubated with AMS, whereas the single-cysteine S220C is labeled at 250 μM FM (data not shown).

Pinpointing the Borderline of the TMD—The length of the TAP1-TMD and its number of TMs are very difficult to predict. In particular, the large C-terminal region from residue 344 to 488 is ill-defined and has been placed outside the TMD (19, 20). To elucidate the membrane topology of this region, we examined the accessibility of three cysteines (T399C, S436C, and S488C) by the membrane-impermeable probe FM (Fig. 4). Semipermeabilized cells were labeled with 50 μM FM for different periods of time (0.5–5 min). For reference, the membranes were permeabilized prior to labeling and treated identically. Cysteines at

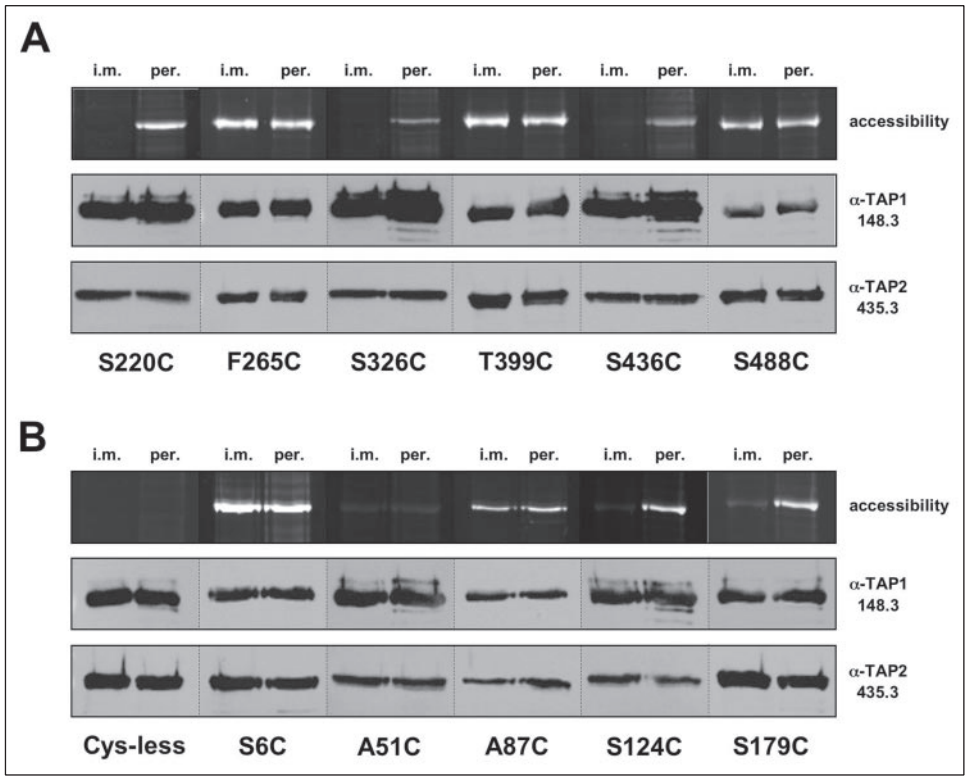

FIGURE 5. **Labeling of single-cysteine constructs.** *A*, labeling of single cysteines within the predicted transport core domain (S220C, F265C, S326C, T399C, S436C, and S488C). *B*, labeling of single cysteines within the predicted N-terminal domain (S6C, A51C, A87C, S124C, and S179C). Cys-less TAP was used as a negative control in the labeling reaction. In addition to intact membranes (*i.m.*), membranes were permeabilized (*per.*) with DM prior to labeling. After labeling with FM (50 μM) and purification of the TAP complex via Ni-NTA-agarose, aliquots were analyzed by SDS-PAGE (10%). FM labeling was monitored by in-gel fluorescence imaging. Co-purification of TAP1 and TAP2 was confirmed by immunoblotting with TAP1- (mAb148.3) and TAP2-specific (mAb435.3) antibodies, respectively.

positions 399 and 488 are equally well accessible and therefore located in the cytosol. Strikingly, the cysteine at position 436 was not labeled in intact intracellular membranes at any time, whereas it could be easily labeled after membrane permeabilization. As a control, the corresponding immunoblot revealed similar expression levels of TAP1 and TAP2. These data clarify conflicting models regarding the structural organization of the TAP complex and demonstrate that residue 436 is sited in an ER-luminal loop and separated by two transmembrane segments from residues 399 and 488, which are located in cytosolic loops. Thus, TAP1 has an unusually large TMD that spans almost 490 residues.

Membrane Topology of the Core Transmembrane Domain—Most recently, a translocation core TMD within TAP1 and TAP2 has been identified, which is sufficient for membrane targeting, heterodimer assembly, peptide binding, and translocation of the transport complex (7, 8). To investigate the membrane topology of this translocation core domain, we generated a set of single-cysteine mutants in the region of residues 179–488 (Fig. 5*A*). For F265C, T399C, and S488C, we detected equal labeling efficiencies with FM in intact membranes as well as permeabilized membranes. These results indicate that residues 265, 399, and 488 are positioned in the cytosol. No labeling was observed for cysteines introduced at positions 220, 326, or 436 in intact membranes, whereas strong labeling was observed after permeabilization of intracellular membranes. These data prove that residue 220, 326, and 436 are located in the ER lumen. Similar expression levels for all TAP constructs were confirmed by immunoblotting. No labeling was detected for Cys-less TAP (Fig. 5*B*), demonstrating that all reactions are site-specific.

Membrane Topology of the N-terminal Domain—Members of the TAP family harbor a unique, extra N-terminal domain, which is not found in P-glycoprotein or any other ABC transporter. This N-terminal domain (residues 1–175 of TAP1 and 1–140 of TAP2) is essential for tapasin binding and assembly of the macromolecular peptide-loading complex (7, 21). To map the membrane topology of this N-terminal domain, we introduced single cysteines at position 6, 51, 87, 124, and 179 of TAP1 (Fig. 5*B*). Similar expression levels for all TAP constructs were confirmed by immunoblotting. For cysteines S6C and A87C, no difference in FM labeling between intact membranes and permeabilized membranes was observed, demonstrating that these residues are located in cytosolic loops. In contrast, construct S124C showed a clear labeling pattern accounting for its ER localization. Surprisingly, the introduced cysteines at positions 51 and 179 (predicted to be in the ER lumen and cytosol, respectively) were not accessible for labeling. For A51C, labeling was not possible under either condition, indicating that this cysteine, although sited in a predicted hydrophilic loop, is hidden within the assembled TAP complex. In the case of S179C, FM labeling was low and slightly weaker in intact membranes than in permeabilized membranes. However, specific cleavage of an epitope tag fused N-terminally to residue 167 of TAP1 (residues 167–748) by a cytosol-resident protease confirmed the cytosolic orientation of this region (Fig. 7 and supplemental material).

Tapasin Binding to the N-terminal Domain Does Not Change Its Membrane Topology—To account for the possibility that tapasin binding might affect the membrane topology of the N-terminal domain, we co-expressed the single-cysteine constructs A51C, A87C, S124C, and S179C together with tapasin (Fig. 6). Co-expression and assembly of TAP1, TAP2, and tapasin were confirmed by affinity purification of TAP1 and immunodetection using specific antibodies to TAP1, TAP2, and tapasin. The accessibility of all single cysteines for FM labeling was not altered by tapasin, indicating that tapasin binding does not change the overall membrane topology of the N-terminal domain.

DISCUSSION

ABC transporters comprise one of the largest protein families, which are abundant among all three phyla of life. Their cellular functions and substrate specificities are diverse and their dysfunctions in humans lead to severe Mendelian diseases, such as cystic fibrosis. To understand how these transporters work, functional and structural information are

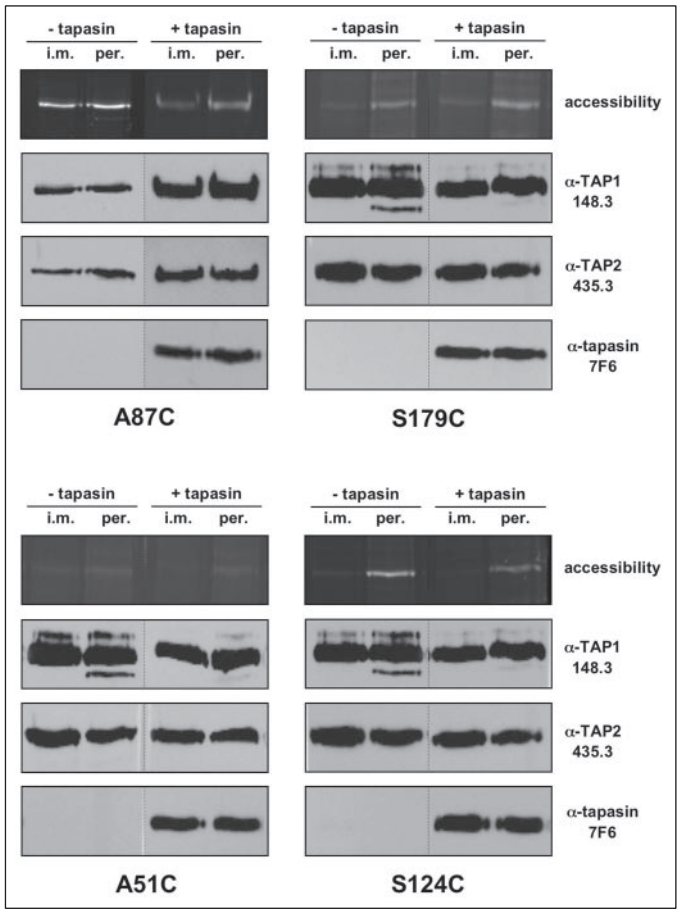

FIGURE 6. **Labeling of single cysteines within a tapasin-TAP complex.** Labeling of single cysteines within predicted cytosolic (A87C and S179C) and ER-luminal loops (A51C and S124C) in the absence (−) and presence (+) of tapasin. In addition to intact membranes (*i.m.*), membranes were permeabilized (*per.*) with DM prior to labeling. After labeling with FM (50 μM) and purification of the TAP complex via Ni-NTA-agarose, aliquots were analyzed by SDS-PAGE (10%). FM labeling was monitored by in-gel fluorescence imaging. Co-purification of TAP1, TAP2, and tapasin was confirmed by immunoblotting with TAP1- (mAb148.3), TAP2- (mAb435.3), and tapasin-specific (7F6) antibodies, respectively.

greatly needed. However, the crystallization of membrane proteins (in particular, eukaryotic multisubunit complexes expressed at low level) is a very difficult task. Certain algorithms can predict the likelihood of a polypeptide to comprise a membrane-spanning α-helix. On the basis of sequence alignments with other ABC transporters of the subfamily B in combination with hydrophobicity plots, 10 and 9 TMs have been predicted for human TAP1 and TAP2, respectively (22, 23). For ABC transporters, however, the prediction is intrinsically difficult, mainly because the hydrophobicity and length of TMs are not well defined.

In the case of experimental approaches, one major drawback has been that non-functional, singly expressed reporter or truncation constructs of TAP subunits were applied (20, 24). Lacking any functional read-out, the authors suggested that a translocation pore is formed by the six and five N-terminal TMs of TAP1 and TAP2, respectively (20, 24). ABC transporters, however, depend on complex intra- and intermolecular helix packing and tight TMD-TMD interactions. Thus, without ensuring the overall integrity of the transport complex, previous results are not very likely to match reality. Consequently, this topology study and prior work disclosing the minimally functional translocation unit (7, 8) disproved the model of an N-terminal pore, demonstrating that the essential translocation pathway is built by six C-terminal TMs of TAP1 (residues 167–488) and TAP2 (residues 123–454).

Over the past decade, extensive studies have been performed to elucidate the membrane topology of primary and secondary transporters employing cysteine-scanning mutagenesis in combination with thiol-specific labeling of single cysteines. This technique proved to be very powerful because the introduction of cysteine residues is minimally invasive and therefore tolerated without affecting the structure and function of the target protein. This method has been very successful in elucidating the membrane topology of *e.g.* the lactose permease (25), the multidrug transporter P-glycoprotein (26), the GAT-1 transporter (27), the glutamate transporter GLT-1 (28), and the MotA protein (29). However, it had not yet been applied to intracellular multicomponent membrane protein complexes.

To decipher the membrane topology of human TAP, we first generated a cysteine-less transport complex by *de novo* gene assembly for subsequent introduction of single cysteines at defined positions. We could demonstrate that the Cys-less heterodimeric TAP complex devoid of 19 cysteines is functional in peptide transport and inhibition by the TAP-specific viral protein ICP47. Based on sequence alignments and hydrophobicity algorithms of TAP from different species and homologous ABC transporters, we introduced single cysteines in predicted transmembrane loops. All TAP1 variants were co-expressed with Cys-less TAP2 and assembled in a functional transport complex. The accessibility of the single cysteines was probed with thiol-specific membrane-impermeable fluorophores in semipermeabilized living cells.

In this study, we have elucidated for the first time the topological organization of transmembrane segments of TAP1 within a functional transport complex. As summarized in Fig. 7, residues 220, 326, and 436 are found in ER-luminal loops, whereas residues 265, 399, and 488 face the cytosol. This region was identified to be essential for ER targeting, heterodimerization, peptide binding, and transport of the TAP complex (7, 8). Based on these results, we conclude that the transporter core is formed by 6 + 6 TMs, which is common for most ABC transporters.

In addition to the 6 + 6 TM core, TAP1 and TAP2 comprise an extra N-terminal domain that is essential for assembly of the peptide-loading complex mediated by the adapter protein tapasin (7). To investigate the membrane topology of this unique N-terminal domain of TAP1 (residues 1–175), we employed the single-cysteine constructs A51C and S124C (ER-luminal residues) as well as S6C, A87C, and S179C (cytosolic residues). Based on the results obtained for the S6C construct, the N terminus is sited in the cytosol. Because the N terminus and the C-terminal nucleotide-binding domain are both located in the cytosol, TAP1 has an even number of transmembrane helices. By hydrophobicity algorithms, four TMs are well predicted for the N-terminal domain of TAP1. Residues 6 and 87 are found to be located in the cytosol and residue 124 in the ER lumen, thus allowing for a precise determination of the membrane topology of the N-terminal domain, which contains four well predicted TMs (Fig. 7).

The topology of residues 51 and 179 could not be defined by cysteine-scanning mutagenesis. Even treatment with different thiol-specific compounds did not improve labeling of these residues. However, specific cytosolic cleavage of an epitope tag fused N-terminally to residue 167 of TAP1 (residues 167–748) confirmed the cytosolic orientation of this region (Fig. 7 and supplemental material). It is interesting to note that two hydrophobicity algorithms, TopPred II (30) and SOSUI (31), annotate the cysteine A51C almost at the start of the second transmembrane helix (Fig. 7). In conclusion, it seems therefore very likely that the two cysteines are hidden within an assembled TAP complex.

Because the N-terminal domain comprises a docking site for tapasin, we questioned whether tapasin binding could trigger structural rearrangements in the TAP complex, which should result in an altered

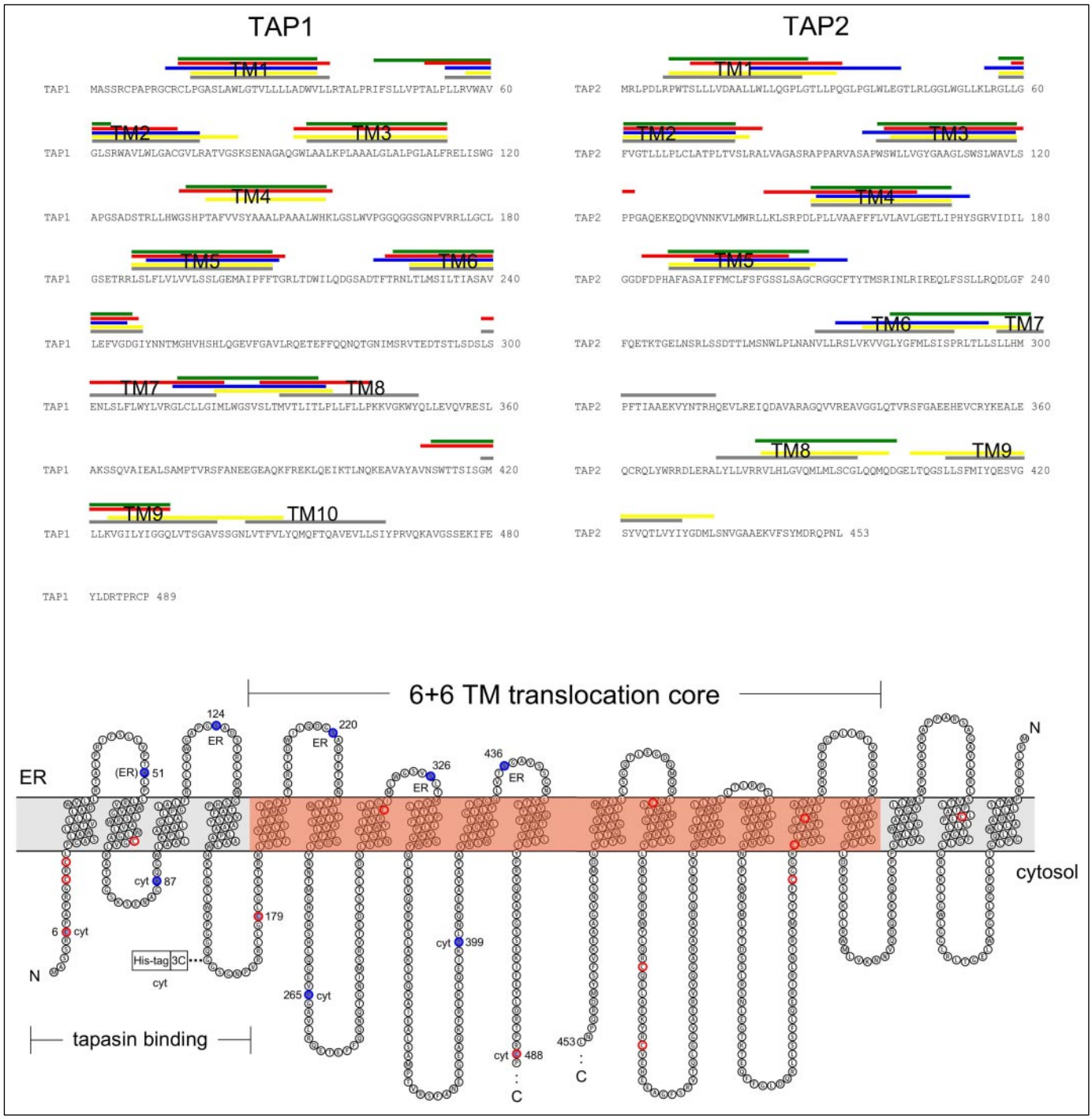

FIGURE 7. **Membrane topology of TAP.** The membrane topology was predicted based on sequence alignments (ClustalW with the human P-glycoprotein and several topology prediction programs: TopPred II (*green bars* (30)), SOSUI (*red bars* (31)), TMHMM (*blue bars* (32)), and TMPred (*yellow bars* (33)). Standard setups for eukaryotic membrane proteins were used for each algorithm. *Gray lines* indicate the data for TMs of human TAP1 and TAP2 derived from the Swiss Protein Data Base (accession numbers Q03518 and Q03519). The TAP complex consists of TAP1 and TAP2, each comprising one TMD and one nucleotide-binding domain (not shown). Each TMD can be subdivided into a unique N-terminal domain essential for tapasin binding and a 6 + 6 TM translocation core (*shaded* in *red*), which is crucial for ER targeting, heterodimerization, peptide binding, and transport. Positions at which single cysteines were introduced and their orientation relative to the membrane are indicated in *blue* and labeled with *ER* or *Cyt*, respectively. Exchanged intrinsic cysteines within each TMD of the Cys-less TAP complex are shown as *red circles*. The position of a protease (*3C*)-cleavable His_{10} tag fused to the N terminus of TAP1 of a mini6TAP complex (7) is indicated.

accessibility of the single cysteines in the N-terminal domains for thiol-specific reagents. We therefore studied the accessibility of single-cysteine constructs S6C, A51C, A87C, S124C, and S179C within an assembled complex of TAP1, TAP2, and tapasin. Surprisingly, tapasin binding did not alter the labeling efficiency of TAP1, indicating that the topology of the N-terminal domain is not affected during the assembly of the peptide-loading complex. This result is supported by the fact that the level of TAP-associated tapasin is in the same range in microsomes of baculovirus-infected *Sf9* cells and Raji cells (data not shown).

As illustrated in Fig. 7, the topology algorithms match very well the first six transmembrane segments of TAP1, with the slight deviation for TM2 as discussed above. However, almost all algorithms failed to pre-

dict TM7/8 and TM9/10, mainly because of their hydrophilic character and very short ER-luminal loops. Only the combination of detailed sequence alignments and topology algorithms favor ten transmembrane helices, which is in agreement with the experimental results.

Based on the sequence identity between human TAP1 and TAP2 (38%, TMD 25%), the membrane topology of TAP2 can be predicted, resulting in nine transmembrane-spanning segments (Fig. 7). The TMD of TAP2 can be subdivided into a transport core domain of six TMs and a unique extra N-terminal domain comprising three TMs. In contrast to TAP1, the N terminus of TAP2 is located within the ER lumen (Fig. 7). Strikingly, the position of the last five TMs of TAP1 and TAP2 are in quite perfect agreement with human P-glycoprotein, indicating a similar structural organization of their translocation cores .

In summary, we have determined the membrane topology of TAP1 within a fully assembled, functional, multicomponent transport complex in the ER membranes of intact cells. This study represents an important step in understanding the structure of the peptide-loading complex.

Acknowledgments—We thank Renate Guntrum, Eckhard Linker, and Nils Richter for excellent technical assistance as well as Klaus Hoffmeier and Michael Schrodt for help in preparing Fig. 7.

REFERENCES

1. Grommé, M., and Neefjes, J. (2002) *Mol. Immunol.* **39,** 181–202
2. Lehner, P. J., and Cresswell, P. (2004) *Curr. Opin. Immunol.* **16,** 82–89
3. Higgins, C. F. (1992) *Annu. Rev. Cell Biol.* **8,** 67–113
4. Schmitt, L., and Tampé, R. (2002) *Curr. Opin. Struct. Biol.* **12,** 754–760
5. Abele, R., and Tampé, R. (2004) *Physiology* (*Bethesda*) **19,** 216–224
6. Beismann-Driemeyer, S., and Tampé, R. (2004) *Angew. Chem. Int. Ed. Engl.* **43,** 4014–4031
7. Koch, J., Guntrum, R., Heintke, S., Kyritsis, C., and Tampé, R. (2004) *J. Biol. Chem.* **279,** 10142–10147
8. Koch, J., Guntrum, R., and Tampé, R. (2005) *FEBS Lett.* **579,** 4413–4416
9. Chang, G., and Roth, C. B. (2001) *Science* **293,** 1793–1800
10. Chang, G. (2003) *J. Mol. Biol.* **330,** 419–430
11. Reyes, C. L., and Chang, G. (2005) *Science* **308,** 1028–1031
12. Locher, K. P., Lee, A. T., and Rees, D. C. (2002) *Science* **296,** 1091–1098
13. Heintke, S., Chen, M., Ritz, U., Lankat-Buttgereit, B., Koch, J., Abele, R., Seliger, B., and Tampé, R. (2003) *FEBS Lett.* **533,** 42–46
14. Chen, M., Abele, R., and Tampé, R. (2004) *J. Biol. Chem.* **279,** 46073–46081
15. Chen, M., Abele, R., and Tampé, R. (2003) *J. Biol. Chem.* **278,** 29686–29692
16. Meyer, T. H., van Endert, P. M., Uebel, S., Ehring, B., and Tampé, R. (1994) *FEBS Lett.* **351,** 443–447
17. van Endert, P. M., Tampé, R., Meyer, T. H., Tisch, R., Bach, J. F., and McDevitt, H. O. (1994) *Immunity* **1,** 491–500
18. Ahn, K., Meyer, T. H., Uebel, S., Sempé, P., Djaballah, H., Yang, Y., Peterson, P. A., Früh, K., and Tampé, R. (1996) *EMBO J.* **15,** 3247–3255
19. Gileadi, U., and Higgins, C. F. (1997) *J. Biol. Chem.* **272,** 11103–11108
20. Vos, J. C., Spee, P., Momburg, F., and Neefjes, J. (1999) *J. Immunol.* **163,** 6679–6685
21. Ortmann, B., Copeman, J., Lehner, P. J., Sadasivan, B., Herberg, J. A., Grandea, A. G., Riddell, S. R., Tampé, R., Spies, T., Trowsdale, J., and Cresswell, P. (1997) *Science* **277,** 1306–1309
22. Tampé, R., Urlinger, S., Pawlitschko, K., and Uebel, S. (1997) in *Unusual Secretory Pathways: From Bacteria to Man* (Kuchler, K., Rubartelli, A., and Holland, B., eds) pp. 115–136, Springer, New York
23. Lankat-Buttgereit, B., and Tampé, R. (1999) *FEBS Lett.* **464,** 108–112
24. Vos, J. C., Reits, E. A., Wojcik-Jacobs, E., and Neefjes, J. (2000) *Curr. Biol.* **10,** 1–7
25. Kaback, H. R., Sahin-Toth, M., and Weinglass, A. B. (2001) *Nat. Rev. Mol. Cell Biol.* **2,** 610–620
26. Loo, T. W., and Clarke, D. M. (1995) *J. Biol. Chem.* **270,** 843–848
27. Bennett, E. R., and Kanner, B. I. (1997) *J. Biol. Chem.* **272,** 1203–1210
28. Grunewald, M., Bendahan, A., and Kanner, B. I. (1998) *Neuron* **21,** 623–632
29. Zhou, J., Fazzio, R. T., and Blair, D. F. (1995) *J. Mol. Biol.* **251,** 237–242
30. von Heijne, G. (2002) *J. Mol. Biol.* **225,** 487–494
31. Hirokawa, T., Boon-Chieng, S., and Mitaku, S. (1998) *Bioinformatics* **14,** 378–379
32. Krogh, A. (2001) *J. Mol. Biol.* **305,** 567–580
33. Stoffel, W., Duker, M., and Hofmann, K. (1993) *FEBS Lett.* **333,** 119–122